Mineral Chemistry of Chlorite Replacing Biotite from Granitic Rocks of the Canadian Appalachians

A.A. Tabbakh Shabani[*]

*Research Center for Earth Sciences, Geological Survey and Mineral Exploration of Iran,
Azadi Square, Meraj Street, PB 13185-1494 Tehran, Islamic Republic of Iran*

Abstract

Chlorite flakes, as a product of alteration of biotite, the dominant ferromagnesian mineral in the Paleozoic granitic rocks of the Canadian Appalachians, have been analyzed by electron microprobe for major elements and by ^{57}Fe Mössbauer spectroscopy for the coordination and oxidation state of Fe. Comparison of Mössbauer Fe^{3+}/Fe ratios obtained from chlorite and its host biotite indicates that chloritization might have occurred under relatively oxidizing conditions. Based on 54 analyzed samples, Si cation totals of these sheet silicates are less than 6.25 atoms per formula unit (apfu), and the sum of octahedral cations is very close to 12 both an indication of trioctahedral chlorite. The calculated mole fraction of chlorite in interlayered phase, *Xc*, ranges from. 0.72 to 0.98 confirming that the chlorites are completely free of any smectite layers. Compositional variations in chlorite are strongly controlled by host biotite and rock type. Fe/(Fe+Mg) ratio ranges from 0.35 to 0.93 and Si contents from 5.18 to 6.11 apfu lead to the classification of chlorites mainly as ripidolite and brunsvigite. All major elements in the chlorite are strongly correlated with each other. Fe/(Fe+Mg) ratio in biotite is well preserved by chlorite. Chlorite thermometry based on the variation in tetrahedral Al content within the chlorite structure shows a large variation in temperatures from 200 to 390 °C with an average of 340 °C. The chlorite from igneous rocks could also be used to detect reheating events and reveal the thermal history of the rocks.

Keywords: Chlorite; Biotite; Alteration; Granite; Appalachian orogen

Introduction

Chlorite is a common and important layer silicate formed under a wide range of conditions. Its crystal structure consists of a T-O-T (tetrahedral-octahedral-tetrahedral) or 2:1 layers (also called talc layers) which are bound together by hydroxide sheets (also called brucite layers). In low to medium grade regional metamorphic rocks, chlorite is one of the most eminent sheet silicates and may be the most abundant mineral in metamorphic rocks of the chlorite zone (e.g. [64, 44, 3, 36, 9, 26, 31, 68, 71, 54, 67, 5, 43, 27, and 37]). In

[*] Corresponding author, Tel.: +98(21)64592285, Fax: +98(21)66070517, E-mail: aatshabani@gmail.com

sedimentary rocks, chlorite is a common, but usually minor component (e.g. [59, 58, 16, and 8]). Occasionally, chlorite makes up the bulk of the clay mineral fraction of sedimentary rocks. Some chlorite is of detrital origin in sediments (e.g., [4]), but some chlorite forms during diagenesis (e.g., [25, 38, and 53]) and some in geothermal systems and hydrothermal ore deposits (e.g. [30, 10, 39, 35, 56, 45, 12, 73, 13, and 72]). In igneous rocks it occurs usually forming secondarily by deuteric or hydrothermal alteration of primary ferromagnesian minerals, such as mica, pyroxene, amphibole, garnet, and olivine. It is a common constituent of altered basic rocks (e.g. [42, 40, and 41]) and hydrothermal alteration zones around ore bodies (e.g., [69, 32, and 57]).

In granitic rocks, chlorite as an alteration product of biotite has attracted the attention of many researchers (e.g., [21, 52, 23, 62, 22, 1, 34, 74, 14, 7, 70, and 60]) to investigate mineralogical features and mechanism of its formation. In addition, chlorite is almost ubiquitous as an alteration product interleaved with, or completely replacing biotite flakes which are found in nearly all types of granites and granitic rocks of the Canadian Appalachians [55]. Likewise, this paper is aimed to provide chemical data on chlorites and to interpret the composition with respect to host biotites and rock types to obtain a better understanding of its occurrence, since no attempt has been made so far to characterize it in these rocks. In this study, we document by electron microprobe the chemical composition of 54 chlorite and host biotite specimens taken from different granitic plutons from the Canadian Appalachian orogen in New Brunswick and Newfoundland provinces. Of these, 10 biotite and 2 chlorite specimens were studied by Mössbauer spectroscopy to document the coordination and oxidation state of iron.

Materials and Methods

Brief Geological Setting

Plutonic rocks comprise about one quarter of all exposed rocks in the Canadian Appalachians. These rocks are granitic in the broad sense, meaning that for the most part they are members of the tonalite to alkali-feldspar granite suite. Much of this granitic plutonism occurred during Middle Ordovician to Early Devonian times [65]. Details of the geological, petrological, geochemical and isotopic characteristics of these suites and plutons have been discussed elsewhere [65, 66, 33, and 17].

Electron Microprobe Analysis

Mineral analyses were obtained by wavelength-dispersive X-ray spectrometry for 11 elements (K, Na, Mg, Ca, Mn, Fe, Al, Ti, Si, F, and Cl) using the JEOL 8900 Superprobe of the McGill University Microprobe Laboratory. Typical beam operating conditions were 15 kV and 20 nA.

Chlorite analyses were carried out simultaneously with the host biotite analyses for each sample, using the same standards. Representative chemical compositions of chlorites are presented in Table (1) along with their respective structural formulae on the basis of $O_{20}(OH)_{16}$ [i.e., based on chlorite formula $Y_{12} Z_8 O_{20} (OH, F, Cl)_{16}$ where Y and Z are octahedral and tetrahedral sites, respectively]. Total iron is represented as FeO and Fe_2O_3 was determined by Mössbauer spectroscopy of two chlorite specimens (nb-19 and nb-136), which were purified further by hand picking under the binocular to obtain pure chlorite flakes; however, interleaved biotite could not be avoided. For the rest of the chlorite samples, Fe_2O_3 values of their host biotites were used for mineral calculations.

Using chemical composition of biotite specimens, structural formulae were calculated based on 20 oxygen atoms and (OH+F+C) = 4. Contents of FeO and Fe_2O_3 for some of the specimens were determined by applying the $Fe^{3+}/(Fe^{2+}+ Fe^{3+})$ ratios determined by Mössbauer spectroscopy (MS). For those samples not measured by MS, the above ratios were extrapolated from those of similar petrographic units. Note that the complete data sets can be obtained from the author upon request.

Mössbauer Spectroscopy

Transmission ^{57}Fe Mössbauer spectra of 12 samples were obtained at room temperature (RT=22°C) using a ^{57}Co rhodium matrix source on a velocity range of ±4 mm/s with a constant acceleration transducer. Data was collected on 1024 channels, which covered twice the Doppler velocity range of ±4 mm/s. Calibrations of spectra were obtained with a ^{57}Fe-enriched iron foil, both before and after each experiment. All positions are reported with respect to this calibration spectrum, i.e., with respect to the centre shift (CS) of metallic -Fe at RT. All spectra were folded to give a flat background (BG).

Absorbers were prepared as follows: Whole rock samples were crushed using both jaw crusher and pulverizer. The crushed samples were then sieved to obtain the size fraction between 45 and 60 mesh (350-250 μm). All samples were washed with water or acetone to remove dust. Magnetite was removed with a

Table 1. Representative electron microprobe analyses of chlorite and their structural formulae based on 28 oxygen atoms from the Canadian Appalachian granites

Sample No.	Nb-195	Nb-189	Nb-30	Nf-52	Nb-29	Nf-78	SNF-4
Mean of analysis points	2	2	4	2	3	2	2
SiO2	27.60	26.79	26.18	25.60	24.78	27.28	25.93
TiO2	0.02	0.04	0.36	0.01	0.06	2.78	0.10
Al2O3	18.64	18.72	18.29	19.41	20.37	15.68	19.79
FeO total	21.11	23.59	31.49	25.08	28.95	28.11	25.00
Fe2O3	4.57	5.11	7.69	5.85	7.39	4.37	3.05
FeO	16.98	18.98	24.54	19.80	22.28	24.17	22.24
MnO	1.01	0.65	1.08	0.93	1.43	0.83	0.96
MgO	18.98	17.42	9.97	16.12	11.72	10.61	16.23
CaO	0.03	0.05	0.09	0.01	0.02	2.52	0.05
Na2O	0.00	0.05	0.02	0.00	0.00	0.02	0.01
K2O	0.03	0.05	0.22	0.01	0.02	0.30	0.06
H2O	11.68	11.46	11.20	11.53	11.31	11.20	11.42
F	0.16	0.30	0.04	0.00	0.03	0.08	0.15
Cl	0.00	0.03	0.00	0.01	0.00	0.01	0.00
total	99.64	99.51	99.66	99.28	99.39	99.81	99.94
Si	5.65	5.55	5.62	5.37	5.28	5.83	5.41
Al	2.35	2.45	2.38	2.63	2.72	2.17	2.59
ΣT site	8	8	8	8	8	8	8
Al	2.15	2.13	2.24	2.16	2.40	1.78	2.28
Ti	0.00	0.01	0.06	0.00	0.01	0.45	0.02
Fe^{+3}	0.70	0.80	1.24	0.92	1.19	0.70	0.48
Fe^{+2}	2.91	3.29	4.41	3.47	3.97	4.32	3.88
Mn	0.18	0.11	0.20	0.17	0.26	0.15	0.17
Mg	5.79	5.38	3.19	5.04	3.73	3.38	5.05
ΣO site	11.75	11.77	11.42	11.77	11.56	11.44	11.91
Ca	0.01	0.01	0.02	0.00	0.00	0.58	0.01
Na	0.00	0.02	0.01	0.00	0.00	0.01	0.00
K	0.01	0.01	0.06	0.00	0.00	0.08	0.02
OH	15.90	15.80	15.97	16.00	15.98	15.94	15.90
F	0.10	0.19	0.03	0.00	0.02	0.06	0.10
Cl	0.00	0.01	0.00	0.00	0.00	0.00	0.00
Fe/(Fe+Mg)	0.38	0.43	0.64	0.47	0.58	0.60	0.46
Xc	0.95	0.95	0.88	0.96	0.92	0.72	0.98

Xc: chlorite component

strong permanent magnet and the mafic and felsic grains were then separated using a Frantz magnetic separator. Further purification in some cases was achieved using heavy liquids (methylene iodide, S.G.= 3.33). Final shaking on a tilted paper sheet and hand-picking were performed for all samples until the concentrates appeared at least 99% pure under the binocular microscope. The amount of sample used in the absorbers varied between 70 to 130 mg and was determined by the method of Rancourt et al. [50] to maximize the signal to noise ratio. The above-mentioned amount of granulated mica corresponding to the ideal (or near-ideal) absorber thickness was then mixed with petroleum jelly in a 5 mm thick and 0.5 inch inside diameter holder. This method has been shown to give random orientation of the mica grains in the absorbers and allows one to impose equality in area of corresponding high and low-energy lines in site-specific doublets [51].

The new Voigt-based model of arbitrary-shape quadrupole splitting distributions (QSD) of Rancourt and Ping [49] was used to fit the spectra. This model assumed that the true underlying QSD for a given valence state and coordination number, i.e., for a given site, is composed of a given number N of Gaussian components as can be justified on statistical grounds and used. Unique distributions are thereby obtained [49].

None of the spectra were thickness corrected, a method which takes into account the spectral distortions that occur because of finite absorber thickness [50, 47, and 48]. Although we know that thickness effects are minimal for these types of absorbers.

Whole-Rock XRF Analyses

Whole-rock major, minor and trace elements were determined by sequential wavelength-dispersive X-ray fluorescence (XRF) with a Philips PW2400 automated spectrometer. Major, minor and trace element analyses were performed on glass discs of fused rock samples.

Results and Discussion

Mössbauer Spectroscopy of Chlorite

Mössbauer spectroscopy (MS) has become a fairly common method for characterizing the local environment of Fe in iron-bearing minerals. It is considered the most precise tool for determination of Fe^{3+}/Fe ratio (e.g. [50]). As natural chlorites usually contain between 5 and 40 weight percents iron, they are considered suitable materials for Mössbauer

spectroscopic investigations [20]. In this study obtained Mössbauer spectroscopy of two chlorite samples have a slightly higher $Fe^{3+}/(Fe^{2+}+Fe^{3+})$ ratio than their host partially chloritized biotite grains. Representative Mössbauer spectrum of a chlorite sample is shown in Figure 1.

All spectra of biotites and chlorites show remarkable similarity and have three main absorption peaks centered at   -0.1, +1.0 and +2.3 mm/s, which respectively correspond to 1) the low-energy lines of both octahedral Fe^{2+} and octahedral Fe^{3+} quadrupole doublets, 2) the high-energy lines of octahedral Fe^{3+} quadrupole doublets, and 3) the high-energy lines of octahedral Fe^{2+} quadrupole doublets. None of these spectra shows a shoulder at 0.4 mm/s corresponding to high energy-lines of quadrupole doublets of Fe^{3+} in tetrahedral sites. This is fully consistent with the calculated structural formulae (Table 1) as there is sufficient Al to completely fill the tetrahedral sites and there is an excess of Al carried over to octahedral sites (1.70-2.78 atoms per formula unit (apfu)). The solid line joining the data points of a given spectrum is the fit result. The other solid lines show the separate contributions from octahedral Fe^{2+} and octahedral Fe^{3+}. The difference spectra (or residuals) are shown with the same vertical scales as the respective spectra.

For instance, the Mössbauer determination of $Fe^{3+}/(Fe^{2+}+Fe^{3+})$ ratio from one specimen of chlorite (nb-136) is 0.23 that is slightly higher than the value of its partially altered parent biotite (0.21), indicating that chloritization of biotite probably occurred under relatively oxidizing conditions.
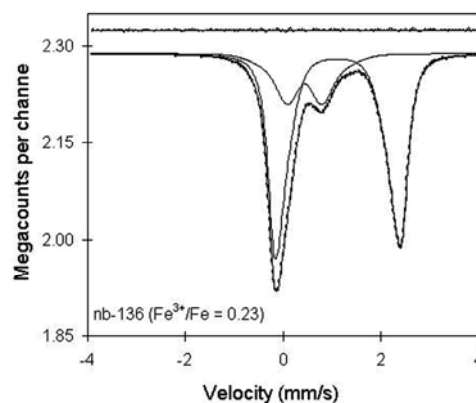

Figure 1. Fitted raw folded spectrum of a representative chlorite sample from granitic rocks of the Canadian Appalachians. The line joining the data points is the fit result. The other solid lines show the separate contributions from octahedral Fe^{2+} and Fe^{3+}. The different spectra are shown with the same vertical scales.

Mineral chemistry of Chlorite

Based on the microprobe data, most of the compositional variations in chlorite reflect large differences in the iron, magnesium, silicon and aluminum contents (Fig. 2). Si and Al are the only constituents of the tetrahedral sheet and the main constituents of the two octahedral sheets are Mg, Fe^{2+}, Al and Fe^{3+} (e.g. Table 1). Fe/(Fe+Mg) ratio ranges from 0.35 to 0.93 and Si contents range from 5.18 to 6.11 apfu lead to the classification of chlorites mainly as ripidolite and brunsvigite (Fig. 3).

Using X-ray diffraction, Bettison and Schiffman [9] identified chlorites from the Coast Range volcanic complex, Troodos ophiolitic rocks, Onikobe and Icelandic geothermal fields that do not have Si cation totals greater than 6.25 cations per 28 oxygens, whereas those with higher values were structurally identified as various interlayered phases such as chlorite-smectite. All our samples except one have Si values less than 6.1 apfu, which is a characteristic indication of chlorite. In addition, according to these investigators Ca value in the structure of chlorite should not be greater than 0.10 cations per 28 oxygens; otherwise indicates the presence of a smectite component. Our 51 samples out of 54 have Ca values less than 0.10 apfu.

Bettison and Schiffman [9] used also a parameter called Xc which means proportion of brucite layers, i.e., mole fraction chlorite in interlayered phase. They assumed if the analyzed phase lies between pure saponite and pure chlorite, the composition is expressed by (K, Na, $Ca_{0.5})_{z-y}$ $^{VI}[(Mg,Fe,Mn)_{6-y}Al_y]$-$^{IV}[Si_{8-z}Al_z]O_{20}$ $(OH)_4$. $x[(Mg,Fe)_6(OH)_{12}]$. Values for x, y, and z are obtained from the above formula by first calculating a proportioning factor (f). The factor can be determined for two different cases: (1) if $z > y$, $f = 16 / [Al + 2Si + 2Ca + K]$ and (2) if $z < y$, $f = 16 / [Al + 2Si-2Ca-K]$. Structural formulae recalculation of interlayered phases on this basis represents a possible technique by which to evaluate the proportions of saponite and chlorite. For analyses representing pure chlorite, Xc will approach one and the exchangeable cations will be near zero. Pure smectite will be represented by analyses in which Xc is zero. Interlayered phases with 1:1 proportions of chlorite and smectite should have Xc near 0.5.

As tetrahedral Al values of our chlorites are greater than the octahedral Al ones, i.e., $z>y$ (Fig. 4), the Xc parameter obtained from microprobe analyses of our chlorites range from 0.72 to 0.98. The calculated values of Xc, empirical quantification of the proportion of smectite layers in the structure, indicate pure chlorite. In addition, López-Munguira1 et al., [40] in their study on chlorites from the Cambrian basic lavas from the SW

Spain calculated the Xc parameter and found a range from 0.81 to 0.98. They examined the same chlorites further by using XRD and HRTEM techniques that confirmed their chlorites were completely free of any smectite layers.
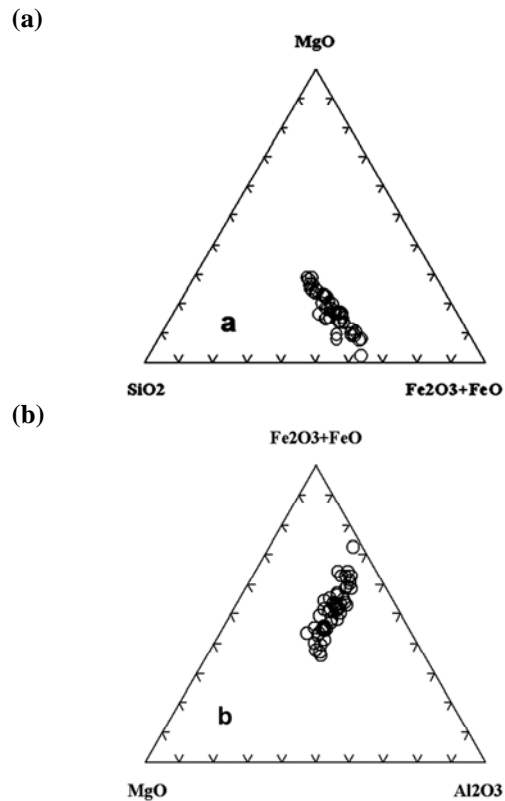
(a)

(b)

Figure 2. (a and b) Compositional variations in chlorite samples from granitic rocks of the Canadian Appalachians based on the contents of iron, magnesium, aluminum and silicon oxides.
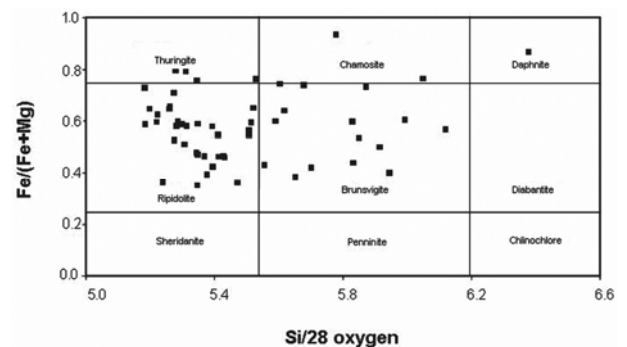

Figure 3. Compositional variations of chlorites in terms of Fe/(Fe+Mg) versus Si (cations/28 oxygen atoms) from granitic rocks of the Canadian Appalachians.

The sum of octahedral cations (11.24-11.90) is very close to 12 in our samples confirming that the chlorite is predominantly trioctahedral, i.e., all octahedral sites are occupied by cations [68]. It is worth mentioning that the chlorite group is subdivided into four subgroups: trioctahedral chlorite, dioctahedral chlorite, di, trioctahedral chlorite and tri, dioctahedral chlorite. Among these, the common form is trioctahedral in both the 2:1 layer and the interlayer hydroxide sheet [6].

Figure 5 exhibits the Fe/(Fe+Mg) ratio of chlorite to that of the biotite precursor. In spite of insignificant degree of scatter, it is evident that there is a strong correlation in the Fe/(Fe+Mg) ratios between chlorite and biotite. This suggests that the iron and magnesium content of chlorite is strongly influenced by the concentration of these elements in the biotite parent. i.e., this ratio is well preserved by the chlorites. The influence of the precursor on the composition of chlorite has also been noted by a number of writers, for instance, Parry and Downey [46], Czamanske et al., [18] and Tulloch, [61]. Likewise, the Fe/(Fe+Mg) chlorite ratio is also dependant on the bulk composition of the host rock (Fig. 6).

Aside from the necessary changes in Si, Al, K, Na, Ca, and H_2O contents, the chlorites differ from their parent biotites in having more magnesium and iron (Fig. 7) and are slightly more oxidized with a higher Fe^{3+} content.

Figure 8, a plot of octahedral Fe^{3+} values versus octahedral Fe^{2+}, displays a general trend that Fe^{2+}-rich chlorites contain more Fe^{3+} than do the Fe^{2+}-poor chlorites. This Fe^{3+} must be considered mainly primary, however a slight degree of oxidation is assumed based on Mössbauer spectroscopy study.

Positive correlation of Mn / Mn + Fe^{2+} between chlorites and parent biotites in Figure 9 exhibits that the majority of chlorites have relatively higher Mn / Mn + Fe^{2+} ratios, i.e., enriched in manganese.

Chlorites contain little of the original Ti content of biotite. TiO_2 values vary from 1.27 to 0.01 (%wt) which is in general not an important constituent of chlorite which probably forms the rutile or titanite intergrown with chlorite.

Calcium, potassium and sodium typically occur as impurities in chlorite [2 and 19]. Czamanske et al., [18] suggested that these elements are, occasionally, absorbed or occur as interlayer cations in chlorite. The depletion of K_2O and decrease in SiO_2 are related to the formation of K-feldspar accompanying the breakdown of biotite to chlorite.

Foster [24] has shown that very few chlorites have total octahedral Al approximately equal to tetrahedral Al. In most cases, octahedral Al is low, and other

trivalent cations, such as Fe^{3+} or Cr^{3+}, are present to proxy for Al in balancing the negative charge on the tetrahedral sheets. If the total number of trivalent octahedral cations is approximately equal to tetrahedral Al, the octahedral occupancy is close to 12.00 atoms. If the total number of trivalent octahedral cations is greater than tetrahedral Al, Foster showed that the total
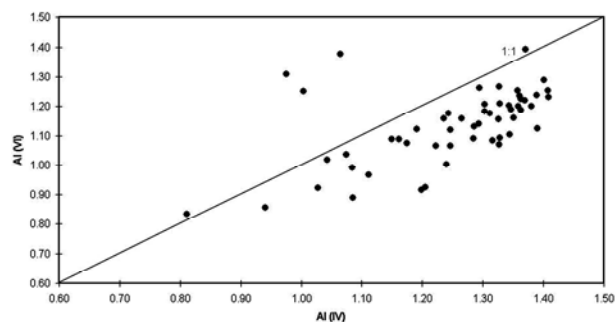

Figure 4. Contents of octahedral Al versus tetrahedral Al in chlorites from granitic rocks of the Canadian Appalachians.
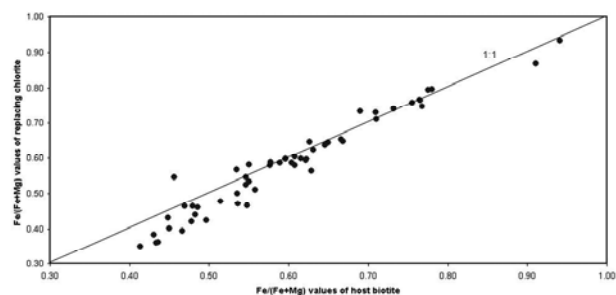

Figure 5. Host biotite Fe/(Fe+Mg) values versus replacing chlorite Fe/(Fe+Mg) contents from granitic rocks of the Canadian Appalachians.
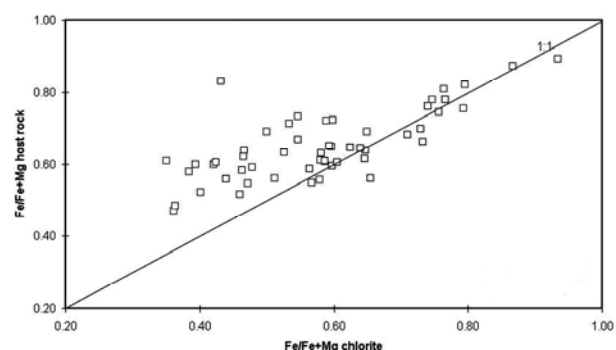

Figure 6. Plot of Fe/(Fe+Mg) value of chlorite samples from granitic rocks of the Canadian Appalachians versus its corresponding value in host rocks.

octahedral occupancy is less than 12.00 atoms by an amount equal to one-half the excess trivalent cations over tetrahedral Al. Structural formula calculations of our chlorites show that the latter case is true (Fig. 3), and this relationship, illustrated also in Figure 10, indicates that the excess trivalent octahedral cations replace divalent cations in the ratio 2:3. Such chlorites have vacancies in the octahedral sites and are called leptochlorites in earlier classifications.

Chlorite thermometry has been developed by several researchers (e.g., [63 and 10]. Here the chlorite thermometer of Cathelineau [10] was used which is based on the variation in tetrahedral Al content within the chlorite structure according to this equation: $T = -61.92 + 321.98 * Al^{IV}$. Calculated temperatures show a large variation temperatures 200 to 390 °C with an average of 340 °C. The range of calculated temperatures seems almost consistent with experimental results obtained by Cole and Ripley [15]. Based on detailed thin section, scanning electron microscope (SEM), x-ray diffraction (XRD), and electron microprobe analyses, these authors demonstrate that biotite is altered exclusively to chlorite in 13 granite-fluid experiments conducted at the following conditions: T = 170–300°C, P = vapor saturation − 200 b, salinity = H2O, 0.1 and 1 m NaCl, fluid/biotite mass ratios = 3−44, run durations = 122−772 h. The amount of chlorite, quantified through point counting and XRD, increased with increasing temperature, salinity, and time.

Figure 11 shows that the majority of our chlorites plot within the field of IIb-structural type. To plot the data on this diagram, structural calculation of chlorite was recalculated on the basis of $O_{10}(OH)_8$ [i.e., based on chlorite formula $Y_6 \, Z_4 \, O_{10} \, (OH, F, Cl)_8$]. The IIb structural type is the most stable chlorite type and occurs mostly in metamorphic rocks and in medium- to high-temperature hydrothermal ore deposits (e.g., [6 and 68]). It is expected that chlorites formed by alteration of pre-existing ferromagnesian minerals in igneous rocks to be of low temperature metastable structural types [6].

What should be the cause, being within the field of IIb-structural type? This can be interpreted in different ways, one possibility, according to Bailey [6], is that at lower temperature chlorite of the higher structural energy can form metastably. This structure may remain indefinitely or, if energy is added to the system through metamorphism, may invert to the stable IIb type. Another possibility is that these chlorites formed in low temperature, as it is expected, but thermal energy of low grade metamorphism caused these low temparture structural type chlorites to convert to more stable IIb structure. It seems that the latter possibility might be true since regional deformation and metamorphism have

affected the Canadian Appalachian rocks at the Silurian (e.g. [65 and 11]).

Based on the data and interpretation presented above it can be concluded that the composition of chlorite, mainly ripidolite and brunsvigite, is closely related to composition of its host biotite. Breakdown of biotite into chlorite was accompanied by the following chemical changes: decrease in SiO_2, K_2O and TiO_2;
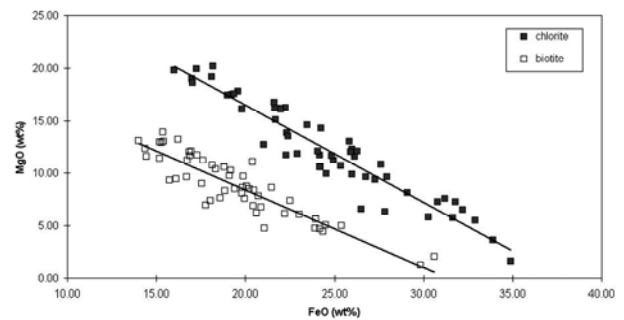

Figure 7. Plot of FeO versus MgO in chlorite samples and their precursor biotite samples from granitic rocks of the Canadian Appalachians.
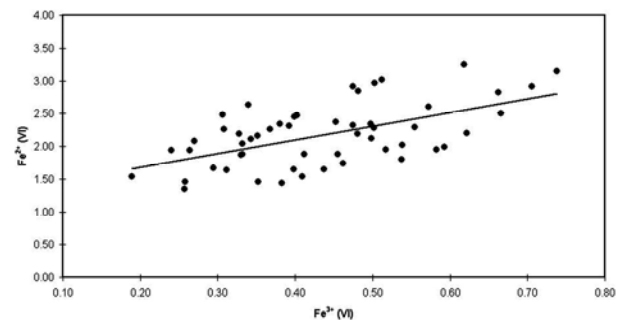

Figure 8. Positive correlation between octahedral Fe^{3+} and Fe^{2+} in chlorite samples from granitic rocks of the Canadian Appalachians.
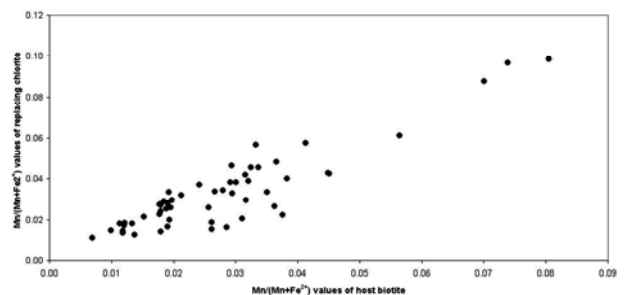

Figure 9. Host biotite $Mn/(Mn+Fe^{2+})$ values versus their replacing chlorite samples from granitic rocks of the Canadian Appalachians.
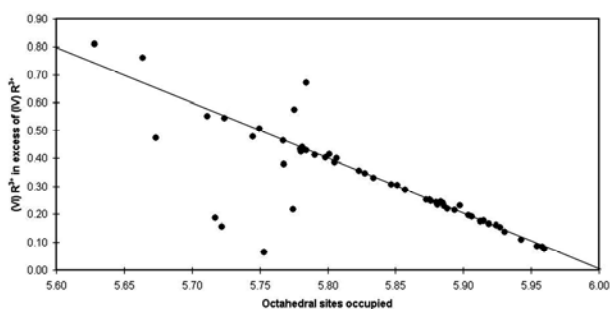
Figure 10. Linear relationship between octahedral cation positions occupied per 6.0 sites and octahedral trivalent cations in excess of tetrahedral trivalent cations in chlorites from granitic rocks of the Canadian Appalachians.
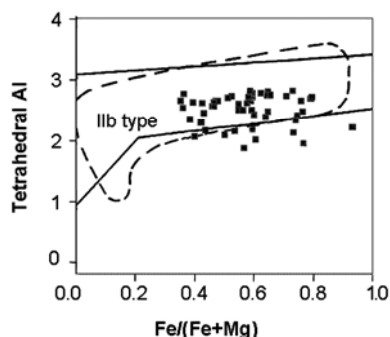

Figure 11. Plot of tetrahedral Al versus Fe/(Fe+Mg) in chlorite samples from granitic rocks of the Canadian Appalachians. The field defined by a solid line is after Hayes (1970) and that defined by dashed line is after Bailey (1988). These two fields define the compositional range of the more stable (IIb structure type) metamorphic chlorite samples.

increase in H_2O, MgO, FeO_{total} and MnO and slight increase in Al_2O_3.

The enrichment of Fe, Mn and Mg in chlorite relative to biotite may be related to structural differences between these minerals.

None of the Mössbauer spectra of chlorite show a shoulder at 0.4 mm/s corresponding to high energy-lines of quadrupole doublets of Fe^{3+} in tetrahedral sites which is completely consistent with the calculated structural formulae. In addition Mössbauer determination of $Fe^{3+}/(Fe^{2+}+Fe^{3+})$ ratios indicate that chloritization of biotite probably occurred under relatively oxidizing conditions.

Our chlorites have total octahedral Al less than tetrahedral Al; therefore, Fe^{3+} is present to proxy for Al in balancing the negative charge on the tetrahedral sheets. However, the total octahedral occupancy is less than 12.00 atoms consequently implying that our

chlorites have vacancies in the octahedral sites.

The studied chlorites are completely free of contamination by smectite layers which is determined by the *Xc* parameter, calculated mole fraction of chlorite in interlayered phase.

Chlorite thermometry shows a large variation in temperatures from 200 to 390 °C with an average of 340 °C which is almost consistent with the experimental results reported on the chloritization of biotite in granitic rocks.

Tetrahedral Al values are remarkably similar to those from the most stable (type IIb) metamorphic chlorite, suggesting, chlorite from igneous rocks could be used to detect the reheating events of the crystalline terrains.

References

1. Abdel-Rahman A. F. Chlorites in a spectrum of igneous rocks: mineral chemistry and paragenesis. Mineralogical magazine, **59**: 129-141 (1995).
2. Albee, A. L. Relationships between the mineral association, chemical composition and physical properties of the chlorite series. American Mineralogist, **47**: 851-870 (1962).
3. AlDahan, A. A., Ounchanum, P. & Morad, S. Chemistry of micas and chlorite in Proterozoic acid metavolcanics and associated rocks from the Hastefalt area, Norberg Ore district, Central Sweden. Contribution to Mineralogy and Petrology, **100**: 19-34 (1988).
4. alonso-Azcárate J. Rodas, M. Barrenechea J. F. and Mas J. R. Clay minerals as provenance indicators in continental lacustrine sequences: the Leza Formation, early Cretaceous, Cameros Basin, northern Spain. Clay Minerals, **40**(1): 79-92 (2005).
5. A´rkai P., Mata M.P., Giorgetti G., Peacor D.R. & To´th M. Comparison of diagenetic and low-grade metamorphic evolution of chlorite in associated metapelites and metabasites: an integrated TEM and XRD study. Journal of Metamorphic Geology, **18**: 531-550 (2000).
6. Bailey, S. W. Chlorites: structures and crystal chemistry, In: Bailey, S. W. (editor) Hydrous Phyllosilicates. Reviews in Mineralogy, **19**: Mineralogical Society of America, Washington DC, 347-403 (1988).
7. Bachliński R. and Smulikowski W. Mineral, whole-rock chemistry and Sr-Nd isotope study of Karkonosze-Kowary gneisses (West Sudetes). Mineralogical Society of Poland – Special Papers, **23**: 29-31 (2003).

8. Barrenechea1 J. F., Rodas M., Frey M., Alonso-Azcárate J. and Mas J. R. Chlorite, corrensite, and chlorite-mica in late jurassic fluvio-lacustrine sediments of the cameros basin of northeastern spain. Clays and Clay Minerals, **48**(2): 256-265 (2000).

9. Bettison, L. A. and Schiffman, P. Compositional and structural variations of phyllosilicates from Point Sal ophiolite, California. American Mineralogist, **73**: 62-76 (1988).

10. Cathelineau M. and Nieva, D. A chlorite solid solution geothermometer The Los Azufres (Mexico) geothermal system. Contribution to Mineralogy and Petrology, **91**: 235-244 (1985).

11. Cawood, P. A., Dunning, G. R., Lux, D. and Van Gool J. A. M. Timing of peak metamorphism and deformation along the Appalachian margin of Laurentia in Newfoundland; Silurian, not Ordovician; with Suppl. Data 9423. Geology, **22**(5): 399-402 (1994).

12. Chabu M. The geochemistry of phlogopite and chlorite from the kipushi zn-pb- cu deposit, Shaba, Zaire. Canadian Mineralogist; **33**(3): 311-325 (1995).

13. Choo, C.O. and Kim, S. J. Occurrence of chlorite and interstratified 7-Å phase in rhyodacitic tuff, southeastern Korea, and implications for hydrothermal alteration conditions. Neues Jahrbuch fur Mineralogie Montshefte, Number **2**: 49-67(19) (2002).

14. Ciesielczuk J. Chlorite from hydrothermally altered strzelin and borów granites (the fore-sudetic block): an attempt of chlorite geothermometry application. Mineralogical Society of Poland – special papers, **20**: 74-76 (2002).

15. Cole D. R. and Ripley E. M. Oxygen isotope fractionation between chlorite and water from 170 to 350°C: a preliminary assessment based on partial exchange and fluid/rock experiments. Geochimica et Cosmochimica Acta, **63**: 449-457 (1999).

16. Curtis, C. D., Hughes, C. R., Whiteman, J. A. and Whittle, C. K. Compositional variation within some sedimentary chlorites and some comments on their origin. Mineralogical Magazine, **49**: 375-86 (1985).

17. Clarke, D.B., MacDonald, M.A. & Tate, M.C. Late Devonian mafic–felsic magmatism in Meguma zone, Nova Scotia. *In* The Nature of Magmatism in the Appalachian Orogen (A.K. Sinha, J.B. Whalen & J. Hogan, eds.). Geol. Soc. Am., Mem., **191**: 107-127 (1997).

18. Czamanske, G. K., Ishihara, S., and Atkin, S. A. Chemistry of rock-forming minerals of the Cretaceous-Paleocene batholith in southwestern Japan and implications for magma genesis. Journal of Geophysical Research, **86**(B11): 10431-10469 (1981).

19. Deer, W. A., Howie, R. A., and Zussman J. Rock-forming minerals, John Wiley and Sons, New York Volume **3**: (1962).

20. De Grave E., Vandenbruwaene J., and Van Bockstael M. ^{57}Fe Mössbauer spectroscopic analysis of chlorite. Physics and Chemistry of Minerals, **15**: 173-180 (1987).

21. Dodge, F. C. W. Chlorites from granitic rocks of the central Sierra Nevada batholith; California. Mineralogical Magazine, **39**: 58-64 (1973).

22. Eggleton, R. A. and Banfield, J. F. The alteration of granitic biotite to chlorite. American Mineralogist, **70**: 902-910 (1985).

23. Ferry, J. M. Reaction mechanisms, physical conditions and mass transfer during hydrothermal alteration of mica and feldspar in granitic rocks from south-central Maine. American Journal of Science, **278**: 1025-56 (1985).

24. Foster, M. D. Interpretation of the composition and classification of the chlorites. USGS Prof Paper **414-A**: 1-33 (1962).

25. Grigsby J.D. Origin and growth mechanism of authigenic chlorite in sandstones of the lower Vicksburg formation, south Texas. Journal of Sedimentary Research, **71**(1): 27–36 (2001).

26. Guidotti, C.V., Teichmann, F. and Henry, D. J. Evidence for equilibrium chlorite in the polymetamorphic metapelites of the Rangeley area, western Maine: American Mineralogist, **76**: 867-879 (1991).

27. Guidotti1 C.V., Sassi F. P., Comodi P., Zanazzi P. F. and Blencoe J. G. Slaty cleavage: does the crystal chemistry of layer silicates play a role in its development? The Canadian Mineralogist; **43**(1): 311-325 (2005).

28. Heyes, J. B. Polytypism of chlorite in sedimentary rocks. Clays and Clay Minerals, **18**: 285-306 (1970).

29. Hey, M. H. A review of chlorites. Mineralogical Magazine, **30**: 276-292 (1954).

30. Innoue, A. and Utada, M. Further investigations of a conversion series of dioctahedral mica/smectite in the Shinzan hydrothermal alteration area, northeast Japan. Clays and Clay Minerals, **31**: 401-12 (1983).

31. Jiang W. W. and Peacor D. R. Prograde transition of corrensite and chlorite in low-grade pelitic rocks from the Gaspe Peninsula, Quebec. Clays and Clay Minerals, **42**: 497 517 (1994).

32. Jiang Y. and Wang R. Mineral chemistry of the Qitianling granitoid and the Furong tin oredeposit in Hunan Province, South China. European Journal of Mineralogy, **17**(4): 635-648 (2005).

33. Kerr, A. Space – time – composition relationships amongst Appalachian-cycle plutonic suites in Newfoundland. *In* The Nature of Magmatism in the Appalachian Orogen (A.K. Sinha, J.B. Whalen, & J. Hogan, editors). Geol. Soc. Am., Mem**, 191**: 193-220 (1997).

34. Kogure T. and banfield J. F. Direct identification of the six polytypes of chlorite characterized by semi-random stacking. American Mineralogist, **83**: 925–930 (1998).

35. Kranidiotis P. Y. and MacLean W. H. Systematics of chlorite alteration at the Phelps Dodge massive sulfide deposit, Matagami, Quebec. Economic Geology, **82**: 1898-911 (1987).

36. Laird J. Chlorites: Metamorphic Petrology. In Hydrous phyllosilicates (exclusive of micas), Bailey S. W. (editor). Mineralogical Society of America, Reviews in Mineralogy, **19**: 405-53 (1988).

37. Lee S. S., Guggenheim S., Dyar M. D. and Guidotti C. V. Chemical composition, statistical analysis of the unit cell, and electrostatic modeling of the structure of Al-saturated chlorite from metamorphosed rocks. American Mineralogist, **92**(5-6): 954-965 (2007).

38. Lindgreen H., Drits V. A., Sakharov, B. A., Jakobsen H. J., Salyn A. L., Dainyak L. G. and Krøyer H. The

structure and diagenetic transformation of illite-smectite and chlorite-smectite from North S *Clay Minerals*; June 2002; v. 37; no. 2; p. 267-281; ea Cretaceous-Tertiary chalk. Clay Minerals, **37**(3): 429-450 (2002).

39. Liou J. G., Seki, Y., Guillemette, R. N. and Saki, H. Compositions and parageneses of secondary minerals in the Onikobe geothermal system, Japan. Chemical Geology, **49**: 1-20 (1985).

40. López-Munguira1 A., Nieto F. and Morata D. Chlorite composition and geothermometry: a comparative HRTEM/AEM-EMPA-XRD study of Cambrian basic lavas from the Ossa Morena Zone, SW Spain. Clay Minerals, **37**(2): 267-281 (2002).

41. Miyahara, M., Kitagawa R. and Uehara S. Chlorite in metabasites from the mikabu and north chichibu belts, southwest japan. Clays and Clay Minerals, **53**(5): 466-477 (2005).

42. Mata M. P., Giorgetti G., Árkai P. and Peacor D. R. Comparison of evolution of trioctahedral chlorite/berthierine/smectite in coeval metabasites and metapelites from diagenetic to epizonal grades. Clays and Clay Minerals, **49**(4): 318-332 (2001).

43. Moazzen M. Chlorite-chloritoid-garnet equilibria and geothermometry in the Sanandaj-Sirjan metamorphic belt, southern IRAN. Iranian Journal of Science and Technology, Transaction A, **28**(A1): 65-78 (2004).

44. Morad S. Mica-Chlorite intergrowths in very low-grade metamorphosed sedimentary rocks from Norway. Neues Jahrb. Mineral. Abh., **154**: 271-87 (1986).

45. Nutt C. J. Chloritization and associated alteration at the Jabiluka unconformity-type uranium deposit, Northern Territory, Australia, Canadian Mineralogist, **27**: 41-58 (1989).

46. Parry, W. T. and Downey, L. M. Geochemistry of hydrothermal chlorite replacing igneous biotite. Clays and Clay Minerals, **30**: 81-90 (1982).

47. Ping J. Y. and Rancourt D. G. Thickness effects with intrinsically broad absorption lines. Hyperfine Interactions, **71**: 1433-1436 (1992).

48. Rancourt D. G. Accurate site populations from Mössbauer spectroscopy. Nuclear Instruments and Methods in Physics Research, **B44**: 199-210 (1989).

49. Rancourt D. G., Ping J. Y. Voigt-based methods for arbitrary-shape static hyperfine parameter distributions in Mössbauer spectroscopy, Nuclear Instruments and Methods in Physics Research, **B53**: 85-97 (1991).

50. Rancourt D. G., McDonald A. M., Lalonde A. E., and Ping J. Y. Mössbauer absorber thicknesses for accurate site populations in iron-bearing minerals. American Mineralogist, **78**: 1-7 (1993).

51. Rancourt D. G., Ping J. Y., and Berman R. G. Mössbauer spectroscopy of minerals III, Octahedral-site Fe^{2+} quadrupole splitting distributions in phlogopite-annite series. Physics and Chemistry of Minerals, **21**: 258-267 (1994).

52. Refaat, Adel. M. and Abdallah, Zeinab M. Geochemical study of coexisting biotite and chlorite from Zaker granitic rocks of Zanjan Area, Northwest, Iran. N.Jb. Miner. Abh., **136**(3): 262-275 (1979).

53. Salem A. M., Ketzer J. M., Morad S., Rizk R. R. and Al-Aasm L. S. Diagenesis and Reservoir-Quality Evolution of Incised-Valley Sandstones: Evidence from the Abu Madi Gas Reservoirs (Upper Miocene), the Nile Delta Basin, Egypt. Journal of Sedimentary Research, 75(4): 572-584 (2005).

54. Schmidt D. and Livi K. J. T. HRTEM and SAED investigations of polytypism, stacking disorder, crystal growth, and vacancies in chlorites from subgreenschist facies outcrops. American Mineralogist, **84**: 160–170 (1999).

55. Shabani, T. A. A., Lalonde A. E., and Whalen J. B. composition of biotite from granitic rocks of the Canadian appalachian orogen: a potential tectonomagmatic indicator? Canadian Mineralogist, **41**: 1381-1396 (2003).

56. Shikazono N. and Kawahata, H. Compositional differences in chlorite from hydrothermally altered rocks and hydrothermal ore deposits. Canadian Mineralogist, **25**: 465-74 (1987).

57. Serafimovski1 T., Dolenec T., and Tasev1 G. Actinolite-phengite-chlorite metasomatites from the Toranica Pb-Zn ore deposit in Macedonia. Materials and Geoenvironment, **53**(4): 445-453 (2006).

58. Srodon, J. and Eberl D. DIllite. In micas, Bailey S. W. (editor). Mineralogical Society of America, Reviews in Mineralogy, **13**: 495-544 (1984).

59. Stoch, L. and Sikora, W. Transformations of micas in the process of kaolinitization of granites and gneisses. Clays and Clay Mineralogy, **24**: 156-62 (1976).

60. Sugimori1 H., Iwatsuki T. and Murakami1 T. Chlorite and biotite weathering, Fe2+-rich corrensite formation, and Fe behavior under low PO2 conditions and their implication for Precambrian weathering. American Mineralogist; **93**(7): 71080-1089 (2008).

61. Tulloch, A. J. Secondary Ca-Al silicates as low-grade alteration products of granitoid biotite. Contribution to Mineralogy and Petrology, **69**: 105-117(1979).

62. Veblen, D. R. and Ferry, J. M. A TEM study of the biotite-chlorite reaction and comparison with petrologic observations. American Mineralogist, **68**: 1160-1168 (1983).

63. Walshe, J. L. A six component chlorite solid solution model and the conditions of chlorite formation in hydrothermal and geothermal systems. Economic Geology, **81**: 681-703 (1986).

64. Weaver, E. R. Shale-slate metamorphism in southern Appalachians. Development in Petrology, **10**: Elsevier, Amsterdam, 239 p. (1984).

65. Whalen J. B. Geology, petrography and geochemistry of Appalachian granites in New Brunswick and Gaspésie, Québec, Geological Survey of Canada, Bulletin **436**: (1993).

66. Whalen, J.B., Jenner, G.A., Longstaffe, F. J., Gariépy, C. & Fryer, B.J. Implications of granitoid geochemical and isotopic (Nd, O, Pb) data from the Cambro-Ordovician Notre Dame Arc for the evolution of the Central Mobile Belt, Newfoundland Appalachians. *In* The Nature of Magmatism in the Appalachian Orogen (A.K. Sinha, J.B. Whalen, & J. Hogan, editors.). Geol. Soc. Am., Mem. **191**: 367-395 (1997).

67. Willner A. P., Hervé F. and Massonne H. Mineral chemistry and pressure–temperature evolution of two

contrasting high-pressure–low-temperature belts in the Chonos Archipelago, Southern Chile. Journal of Petrology, **41**(3): 309-330 (2000).

68. Xie X., Byerly G. R. and Ferrell R. E. IIb trioctahedral chlorite from Barberton greenstone belt: crystal structure and rock composition constraints with implications to geothermometry, Contribution to Mineralogy and Petrology, **126**: 275-291 (1997).

69. Yongfu A. and Guoping L. The Study of Chlorite at Dajing Deposit in Innrer-Mongolia of China. Acta Scientiarum Naturalium Universitatis Pekinensis, **34**(1): 97-105 (1998).

70. Zanazzi P.F., Montagnoli M., Nazzareni S. and Comodi P. Structural effects of pressure on monoclinic chlorite: A single-crystal study. American Mineralogist; Vol. **92**(4): 655-661 (2007).

71. Zane A., Sassi R. and Guidotti C. V. New data on metamorphic chlorite as a petrogenetic indicator mineral, with special regard to greenschist-facies rocks. Canadian Mineralogist, **36**(3): 713-726 (1998).

72. Zagorsky V. Y., Peretyazhko I. S., Sapozhnikov A. N., Zhukhlistov A. P., and Zvyagin B. B. Borocookeite, a new member of the chlorite group from the Malkhan gem tourmaline deposit, Central Transbaikalia, Russia. American Mineralogist, **88**: 830-836 (2003).

73. Zang W. and Fyfe W.S. Chloritization of the hydrothermally altered bedrock at Igarape´ Bahia gold deposits, Caraja´s, Brazil. Mineralium Deposita, **30**: 30-38 (1995).

74. Zieglerand K. Longstaffe F. J. Multiple episodes of clay alteration at the precambrian/paleozoic unconformity, Appalachian basin: isotopic evidence for long-distance and local fluid migrations. Clays and Clay Minerals, **48**(4): 474-493 (2000).